eFood

WILEY

RESEARCH ARTICLE OPEN ACCESS

Edulitin 2, a Ribotoxin-Like Protein From *Boletus edulis* That Triggers Apoptosis in Colon Cancer Cells While Preserving the Integrity of the Intestinal Microbiota

Massimo Bortolotti[1] | Sara Ragucci[2] | Federica Falà[1] | Anella Saggese[3] | Francesco Biscotti[1] | Ylenia De Luca[3] | Nicola Landi[2,4] | Paolo V. Pedone[2] | Andrea Bolognesi[1] | Ezio Ricca[3] | Letizia Polito[1] | Antimo Di Maro[2]

[1]Department of Medical and Surgical Sciences-DIMEC, Alma Mater Studiorum - University of Bologna, Bologna, Italy | [2]Department of Environmental, Biological and Pharmaceutical Sciences and Technologies (DiSTABiF), University of Campania 'Luigi Vanvitelli', Caserta, Italy | [3]Department of Biology, 'Federico II' University, Naples, Italy | [4]Institute of Crystallography, National Research Council, Caserta, Italy

Correspondence: Letizia Polito (letizia.polito@unibo.it) | Antimo Di Maro (antimo.dimaro@unicampania.it)

Received: 29 December 2025 | **Revised:** 13 February 2026 | **Accepted:** 2 March 2026

Funding: PRIN2022 PNRR-MUR, Grant/Award Number: P2022YERKR; ITACA.SB MUR, Grant/Award Number: IR0000009

Keywords: anti-tumor | apoptosis | edible mushrooms | gut microbiota | porcini | ribotoxin-like proteins (RL-Ps)

ABSTRACT

Porcini (*Boletus edulis* Bull.) are a reservoir of pharmacological biomolecules with health-promoting properties. Here, we investigated the cytotoxic activity of edulitin 2, a ribotoxin-like protein purified from *B. edulis* fruiting bodies, against two human colon cancer cell lines (Caco-2 and HT29), and assessed its potential impact on gut microbiota. Edulitin 2 exhibited marked cytotoxicity toward both cell lines in a dose- and time-dependent manner. The effect was particularly evident after 72-h, with EC_{50} values in the 10^{-7} M range for both cell lines. Moreover, edulitin 2 significantly affected barrier integrity in Caco-2 monolayer models. Edulitin 2 kills cells mainly by triggering apoptotic mechanisms, with limited involvement of necroptosis and absence of necrosis. These results support edulitin 2 as a potential therapeutic agent due to the reduced risk of inducing inflammation-related damage. Furthermore, this toxin proved to be harmless to microbial consortia simulating the gut microbiota. Overall, these findings make edulitin 2 a promising bioactive compound that combines cytotoxicity toward colorectal tumor cells with microbiota compatibility. This dual profile supports its further exploration in preclinical models (for loco-regional treatment and as payload of immunotoxins) and highlights the potential of edible mushrooms as a source of novel ribotoxin-like proteins with biomedical relevance.

1 | Introduction

Boletus edulis Bull., known as the king bolete (porcini), is an edible mushroom native to Europe that has since spread to all temperate regions of the Northern Hemisphere (Hall et al. 1998; Sitta and Floriani 2008). Pliny the Elder's writings refer to a mushroom called 'boletus' (then classified as *B. edulis*), consumed by ancient Romans for its flavor, nutritional value and medicinal properties (Hobbs 2021; Tan et al. 2022).

Recently, *B. edulis* has gained popularity as a rich source of nutrients (e.g. raw proteins, essential amino acids, unsaturated fatty acids, dietary fibers, vitamins and key minerals) and for its pharmacological benefits, given that it contains several biomolecules with health-promoting properties (Casado-Hidalgo et al. 2025; Quero et al. 2024). Indeed, *B. edulis* continues to be consumed as traditional food (Central Europe and especially Northern Italy) due to its antioxidant, hepatoprotective, immunomodulatory, antiviral, antimicrobial, antiparasitic,

Massimo Bortolotti and Sara Ragucci share equal first authorship.

Letizia Polito and Antimo Di Maro share equal senior authorship.

anti-hypercholesterolemic and anti-diabetic properties (Casado-Hidalgo et al. 2025; Sivamaruthi et al. 2024; Tan et al. 2022). Furthermore, several studies highlight that *B. edulis* fruiting bodies are a rich reservoir of anti-tumor compounds, which prevent oxidative stress or induce apoptosis. Most of them are polyphenols, flavonoids, terpenoids, polysaccharides (β-glucans) and a specific extract rich in ribonucleic acid (Lemieszek et al. 2019), either separated or as mixtures (Casado-Hidalgo et al. 2025; Lemieszek et al. 2017; Tan et al. 2022). On the other hand, also some proteins isolated from *B. edulis* fruiting bodies were characterized for their anti-proliferative activity against tumor cells. They include: i) two lectins (BEL and BEL β-trefoil) with antineoplastic properties that selectively bind to specific monosaccharides and disaccharides (Bovi et al. 2011; Bovi et al. 2013); ii) a hemagglutinin with antiproliferative activity towards hepatoma (Hep G2) and mouse lymphocytic leukemia cell lines (Sun et al. 2014); iii) an anti-tumor protein (BEAP) that exhibits anti-cancer activity on A549 cell lines both *in vitro* and *in vivo*, by inducing apoptosis and arresting cells in the G1 phase of the cell cycle (Zhang et al. 2021); and, iv) edulitin 2, a ribotoxin-like protein that displays cytotoxic effects against HeLa and HepG2 cell lines triggering the apoptotic pathway (Landi et al. 2021). Among these proteins, only edulitin 2 possesses enzymatic activity; it is a 14-kDa specific ribonuclease belonging to the ribotoxin-like protein (RL-P) family that damages the large ribosomal RNA (Landi et al. 2021).

RL-Ps have been found in most edible basidiomycete mushrooms (Landi et al. 2017; Ragucci et al. 2021), which are commonly consumed for their flavor, nutritional value and nutraceutical properties (Mayirnao et al. 2025). These enzymes are analogous to ribotoxins (e.g. α-sarcin), which are specific extracellular ribonucleases isolated from ascomycetes (Martínez-Ruiz et al. 2001). Both enzyme families have the same target substrate, the α-Sarcin Ricin Loop (SRL) (Herrero-Galán et al. 2013; Olombrada et al. 2017), and cleave a single phosphodiester bond within the SRL of the large rRNA, a conserved hairpin-like structure that interacts with eukaryotic elongation factors (Correll et al. 1998; Wool et al. 1992). The cleavage of the SRL causes a structural change that prevents ribosomes from interacting with elongation factors, thereby irreversibly blocking translation (Szewczak et al. 1993). Although the physiological role of these ribonucleases is still not clear, experimental evidence suggests that they take part in the defense against antagonistic fungi, insects and other pathogens (Landi et al. 2022; Olombrada et al. 2014; Tayyrov et al. 2019). In this context, it is of interest to gain insight into the biological role of these enzymes, investigating their biotechnological applications, considering their potential use as tools in agriculture (e.g. biopesticides) and biomedicine (e.g. targeted therapeutic agents) (Olombrada et al. 2017; Ragucci et al. 2021; Tayyrov et al. 2019).

Thus, given the high specificity of edulitin 2 for its ribosomal target and the high resistance to digestive proteolytic enzymes (Landi et al. 2021), we investigated edulitin 2 toxicity towards two human colon cancer cell lines: Caco-2 and HT29. In addition, considering the potential use of this enzyme (both independently for loco-regional treatment and as part of immunotoxins or nanoconstructs) (Polito et al. 2016; Sharma et al. 2022) in the treatment of colon neoplasms, we evaluated the impact of edulitin 2 on the human gut microbiota *in vitro*.

2 | Materials and Methods

2.1 | Materials

The chemicals for chromatography were previously reported (Landi et al. 2021; Ragucci et al. 2021). The nuclease-treated rabbit reticulocyte lysate system was purchased from Promega (Madison, WI, USA), while *Escherichia coli* ribosomes (New England Biolabs) from Euroclone S.p.A (Pero, Milan, Italy). Other chemicals (analytical grade) were from Sigma-Aldrich Solutions (Merck Life Science, Milan, Italy).

2.2 | Protein Purification

Edulitin 2 was obtained as previously reported (Landi et al. 2021), starting from *B. edulis* fruiting bodies and using a general protocol for the purification of RL-Ps (Ragucci et al. 2021). Briefly, the crude soluble proteins extracted from *B. edulis* fruiting bodies were clarified by acid precipitation and subjected to three sequential chromatographic steps: (i) stepwise cation exchange chromatography to select basic proteins; (ii) gel filtration chromatography (~14-kDa globular proteins separation); and (iii) cation exchange chromatography. Purified edulitin 2 was pooled, dialyzed against water, freeze-dried and stored at −20°C until use. Moreover, ageritin from *C. aegerita* fruiting bodies was purified as previously reported (Landi et al. 2017) and used as a marker of Endo's fragment.

2.3 | Analytical Methods

Protein purity was checked by: (i) SDS-PAGE (Bio-Rad, Milan, Italy) using a 6.0% stacking and 15% separating polyacrylamide gel with and without reducing agent, and (ii) RP-HPLC using a BioBasic-4 column (150 mm × 4.6 mm, 5 μm particle size; Thermo Fisher Scientific, Waltham, MA, USA). For RP-HPLC, the following solvents were used: solvent A (Milli-Q water + 0.1% TFA); and solvent B (acetonitrile + 0.1% TFA). Protein was loaded into the column equilibrated at 95% of solvent A, and eluted using an increasing linear gradient of solvent B, from 5% to 65% of B over 60 min, 1.0 mL/min. Peak elution was monitored at 214 nm (Chambery et al. 2007). The protein concentration was determined by Pierce BCA Protein Assay Kit (Life Technologies Italia Fil., Monza, Italy).

2.4 | Endo's Assay

The release of α-fragment was evaluated by Endo's assay as previously described with a few modifications (Landi et al. 2025). Briefly, *T. harzianum* S30 supernatants (100 μL) or *E. coli* ribosomes [50 μg in 100 μL TMKB buffer 1× (10 mM Tris-acetate, pH 7.6, containing 14 mM Mg-acetate, and 60 mM K-acetate); final concentration 0.22 μM] were incubated with edulitin 2 (5.0 μg; 3.6 μM) for 1 h at 30°C. The same amount of ageritin, the prototype of RL-Ps from *C. aegerita* was used as a positive control, while the substrate incubated without enzyme was used as a negative control. At the end of treatment, RNA was extracted by phenolization and precipitated with cold ethanol. RNA aliquots (4.0 μg) were subjected to 7.0 M urea/5% (w/v) polyacrylamide gel electrophoresis at 15 mA for ~1.5 h and stained for 30 min with the fluorescent nucleic acid stain GelRed (10,000× water) diluted 1:3,300 (v:v) in water (Merck Life Science).

2.5 | Cell Maintenance

Human colon adenocarcinoma cell lines Caco-2 (lot number 300137-220424) and HT29 (lot number 300215-921) were obtained from Cytion (Eppelheim, Germany). Cells were grown in complete medium, consisting of Eagle's minimum essential medium (EMEM), supplemented with 2 mM L-glutamine, 10% (v/v) heat-inactivated fetal bovine serum (FBS), 1% (w/v) non-essential amino acids (100×), 100 U/mL penicillin G and 100 μg/mL streptomycin (Sigma Aldrich, Saint Louis, Dorset, MO, USA). Cells were maintained at 37°C in a humidified atmosphere containing 5% CO_2 in a HeraCell incubator (Heraeus, Hanau, Germany). The culture medium was changed every 2–3 days and cells were regularly split at 90% confluence. All cell lines were routinely tested to confirm the absence of mycoplasma contamination.

2.6 | Cell Viability

Cell viability was assessed using the MTT Cell Growth Assay Kit (Merck). Caco-2 and HT29 were seeded at a density of 3×10^3/well in 96-well microtiter plates (Falcon, Mexico City, Mexico). Following a 24 h-incubation, cells were treated with scalar concentrations of edulitin 2 (ranging from 10^{-10} to 3×10^{-5} M) for 24, 48, 72 h at 37°C. The tested edulitin 2 concentration range was chosen to evaluate cell viability in both sub-toxic and cytotoxic conditions. These concentrations are consistent with those commonly used *in vitro* studies with other ribotoxins. It should be noted that some of these concentrations (until 10^{-6} M) could be achieved in vivo eating porcini, considering that i) 0.76 mg (about 5×10^{-7} M) of edulitin 2 are present in 100 g of fresh raw porcini mushrooms and ii) edulitin 2 is highly resistant to proteolytic enzymes and temperature (Landi et al. 2021). After the indicated time points, the culture medium was removed and replaced with 100 μL/well of fresh medium and 10 μL/well of kit were added. After a 2 h-incubation at 37°C, 100 μL/well of isopropanol, 0.04 M HCl were added in order to dissolve the formazan. Within 1 h, the absorbance at 570 nm was measured by the microtiter plate reader Multiskan EX (ThermoLab systems, Waltham, MA, USA). Each experiment was performed in triplicate. The half maximal effective concentration (EC_{50}), representing the concentration of edulitin 2 required to reduce cell viability by 50% was calculated by linear regression analysis (Bortolotti, Zanello, et al. 2023).

2.7 | Measurement of Transepithelial Electrical Resistance (Teer)

Caco-2 monolayer: Cells (6.25×10^4 cells/cm^2/insert) were seeded on the apical chamber of Transwell inserts in 24-well plates (0.4 μm PET pore membrane, Falcon).

Caco-2/collagen model: Transwell inserts were pre-coated with 0.1 μg/ml of type 1 collagen (Corning, New York, NY, USA) in complete medium and incubated for 1 h at 37°C. At the end of incubation, Caco-2 cells (6.25×10^4 cells/cm^2/insert) were seeded on the apical compartment. In both models, cells were cultured at 37°C in a humidified atmosphere containing 5% CO_2 with complete medium (0.3 mL on the apical side and 0.9 mL on the basolateral side) changed every 2–3 days.

The integrity of the intestinal barrier models is commonly evaluated using Transepithelial Electrical Resistance (TEER) measurements. Edulitin 2 (10^{-6} M) was added to cell layers once TEER reached values ≥ 500 $\Omega \times cm^2$, approximately after 10 days. TEER was subsequently measured at different time-points using a Millicel® ERS 3.0 digital voltohmmeter (Merck) as previously described (Biscotti et al. 2025).

2.8 | Evaluation of Edulitin 2-Induced Cell Death Mechanism

To determine the cell death mechanism induced by edulitin 2 (apoptosis, necroptosis and/or necrosis), Caco-2 and HT29 cells were treated with edulitin 2 and subsequently stained with Annexin V- Enhanced Green Fluorescent Protein (EGFP)/propidium iodide (PI) as previously described (Bortolotti, Biscotti, et al. 2023). Flow cytometry analysis was performed to quantify the distribution of cell death population. This method allows for the discrimination between cells in necrosis (PI-positive and Annexin V-EGFP-negative), in late apoptosis/necroptosis (PI-positive and Annexin V-EGFP-positive) and in early apoptosis (PI-negative and Annexin V-EGFP-positive) (Pietkiewicz et al. 2015). Briefly, cells (4×10^5/well) were seeded in 6-well plates (Corning) and incubated with 10^{-6} M edulitin 2 for 48 h. Cells were then collected, pelleted, washed twice in cold PBS and resuspended in 300 μL of binding buffer, containing Annexin V-EGFP (3 μL) and PI (3 μL). After 10 min incubation in the dark at room temperature, cells were analyzed by the flow cytometer CytoFLEX S (Beckman Coulter, Brea, CA, USA), using the CytExpert Software (version 2.4.0.28, 2011–2019). The involvement of apoptosis in Caco-2 cells was confirmed by a further experimental set, in which cells were pre-treated with the pan-caspase inhibitor Z-VAD (100 μM) 3 h before edulitin 2 intoxication. Apoptosis was then determined by Annexin V-EGFP/PI staining, as above described.

The protective effect of Z-VAD and of the necroptosis inhibitor necrostatin-1 (NEC) was evaluated through cell viability. Caco-2 cells (3×10^3/well) were seeded in 96-well microtiter plates. After 24 h, cells were pre-treated for 3 h with 100 μM Z-VAD or 100 μM NEC, followed by 72 h edulitin 2 (10^{-6} M) treatment. Inhibitors were added to cells every 24 h. Cell viability was assessed as above described.

2.9 | Effects on Intestinal Microorganisms

The impact of edulitin 2 on gut microorganisms was assessed by comparing their growth with or without the ribotoxin-like protein. Gram-negative (*Salmonella enterica typhi* ATCC 1402, *Escherichia coli* DH5α) and Gram-positive (*Bacillus cereus* MV19, *B. subtilis* PY79 and *Lactobacillus rhamnosus* GG) were cultivated in LB broth (8 g/L NaCl, 10 g/L tryptone, 5 g/L yeast extract) at 37°C in shaking condition. Different species of *Candida* (*C. albicans* ATCC 14028, *C. glabrata* and *C. parapsilosis*, intestinal isolates gift of A. Tavanti from the University of Pisa) were cultivated in Potato Dextrose broth (BD Difco, Franklin Lakes, NJ, USA) at 37°C in shaking condition, overnight. Edulitin 2 (1.43×10^{-5} M; 200 μg/mL) was added to the cultures and the growth was monitored

through measurements overtime with a micro-plate reader device (Synergy HTX) in parallel with a control culture not supplemented with the toxin. The experiments were conducted in triplicate.

The effects of edulitin 2 on intestinal microbial consortia were evaluated as previously described (Landi et al. 2025). In summary, fecal samples, collected from children aged 4 to 7 years under sterile conditions, were used for total DNA extraction with the *QIAamp Fast DNA Stool Mini Kit* (QIAGEN S.r.l., Milan, Italy), as previously described (Buglione et al. 2022). DNA yield and integrity were determined using the NanoDrop ND-2000 (NanoDrop, Wilmington, DE, USA) and the Qubit 3.0 Fluorometer (Thermo Fisher Scientific). Each sample was divided into two parts: one aliquot was used directly for total DNA extraction using the same kit, while the other was serially diluted in Modified Gifu Anaerobic Medium [MGAM; Nissui, Tokyo, Japan; (Rettedal et al. 2014)] up to 10^{-8} following the procedure previously reported (Landi et al. 2025). The samples were then incubated anaerobically at 37°C for 3 days in an anaerobic chamber (PLAS LABS, INC. 810-series; Lansing, MI, USA) to allow bacterial growth. The 10^{-4} dilution, representing an intermediate growth phase, was divided into two groups: a treated group, exposed to edulitin 2 (2.86×10^{-5} M; 400 μg/mL), and a control group, without the RL-P. Both cultures were further incubated anaerobically at 37°C for 3 days and subsequently used for total DNA extraction prior to 16S rRNA gene sequencing.

2.10 | Sequencing, Bioinformatics and Statistical Analyses of 16S rRNA Gene Sequences

The taxonomic composition and diversity of the microbial communities were assessed through 16S rRNA gene amplification of the V3 region using the primers Probio_Uni (5′-CCTACGGGRSGCAGCAG-3′) and Probio_Rev (5′-ATTACCGCGGCTGCT-3′) and subsequently sequenced on the Illumina MiSeq platform at GenProbio S.r.l. (University of Parma, Italy; www.genprobio.com). All raw sequences were imported into R and processed using the DADA2 package (Callahan et al. 2016). In accordance with the package guidelines, quality profiles were inspected, and low-quality reads were trimmed using the filter and Trim comand [truncLen = c(260,190), maxN = 0, maxEE = c(2,2), truncQ = 2, rm. phix = TRUE, trimLeft = c(20,21)]. Paired-end reads were merged, and exact Amplicon Sequence Variants (ASVs) were inferred using the dada algorithm. Chimeric sequences were removed, and taxonomic assignment of prokaryotic sequences was performed using the naive Bayesian classifier implemented in QIIME2, with the latest version of SILVA database (138.2) as reference. The obtained sequences are available in the NCBI Sequence Read Archive (SRA) database under the bioproject number PRJNA1291050. Bio-Sample accession number for each sequence is included in Table S1.

Alpha diversity metrics, including the observed number of ASVs, Chao1 richness, and Shannon diversity indices, were calculated to evaluate within-sample diversity. Unpaired Student's *t*-test was used to determine statistical differences of alpha diversity. Beta diversity, representing differences in microbial community composition among samples, was analyzed using Principal Coordinates Analysis (PcoA). GraphPad Prism 9 (San Diego, CA; USA) was used as statistical software.

2.11 | Statistical Analysis

Statistical analysis to evaluate the results of antifungal growth was performed using GraphPad Prism software, version 8 (GraphPad Software, La Jolla, CA, USA). The results from antifungal activity were statistically analyzed using two-way ANOVA test followed by Tukey's multiple comparison test. Normally distributed data were represented as mean ± S.E.M. The significance was accepted for $p < 0.05$. Statistical analyses to evaluate cell viability and the protective effects of cell death inhibitors were conducted using XLSTAT-Pro Software, version 6.1.9, 2003 (Addisoft Inc., Brooklyn, NY, USA). The results are presented as means ± S.D. of three different experiments. The data were analyzed using ANOVA/Bonferroni test or Mann–Whitney *U* test. Dunnett's test was used in addition to ANOVA, when necessary.

3 | Results

3.1 | Edulitin 2 Is Purified From *B. edulis* Fruiting Bodies

The purification of edulitin 2 was achieved according to a procedure previously reported (Landi et al. 2021). The enzymatic activity of edulitin 2 was ascertained by evaluating the ability to release the α-fragment, enzymatic hallmark of RL-Ps, by rabbit reticulocytes *in vitro* through Endo's assay (data not shown), while its purity was assessed by RP-HPLC and SDS-PAGE (Figure 1).

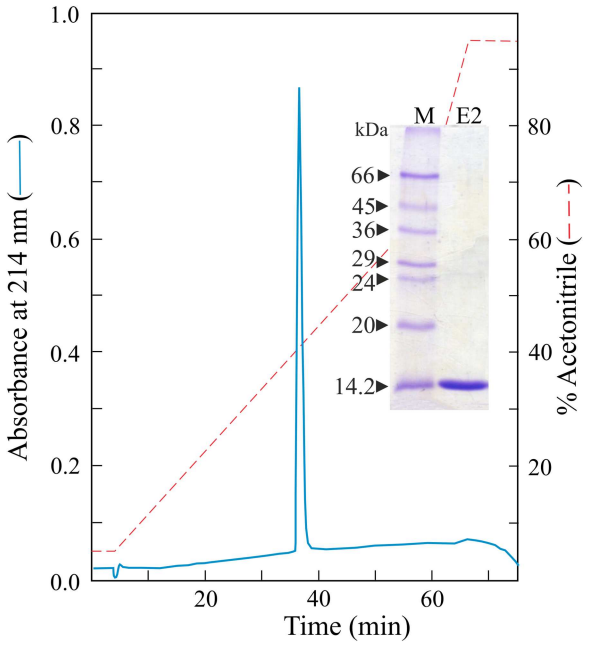

FIGURE 1 | Purity of edulitin 2 preparations. Elution profile of edulitin 2 (100 μg) from a RP-HPLC system by using a BioBasic-4 analytical column. In the insert, SDS-PAGE analysis of edulitin 2 (lane E2; 3.0 μg) in the presence of β-mercaptoethanol (under reducing conditions). Lane M, molecular weight markers. SDS-PAGE was carried out in 12% polyacrylamide separating gel.

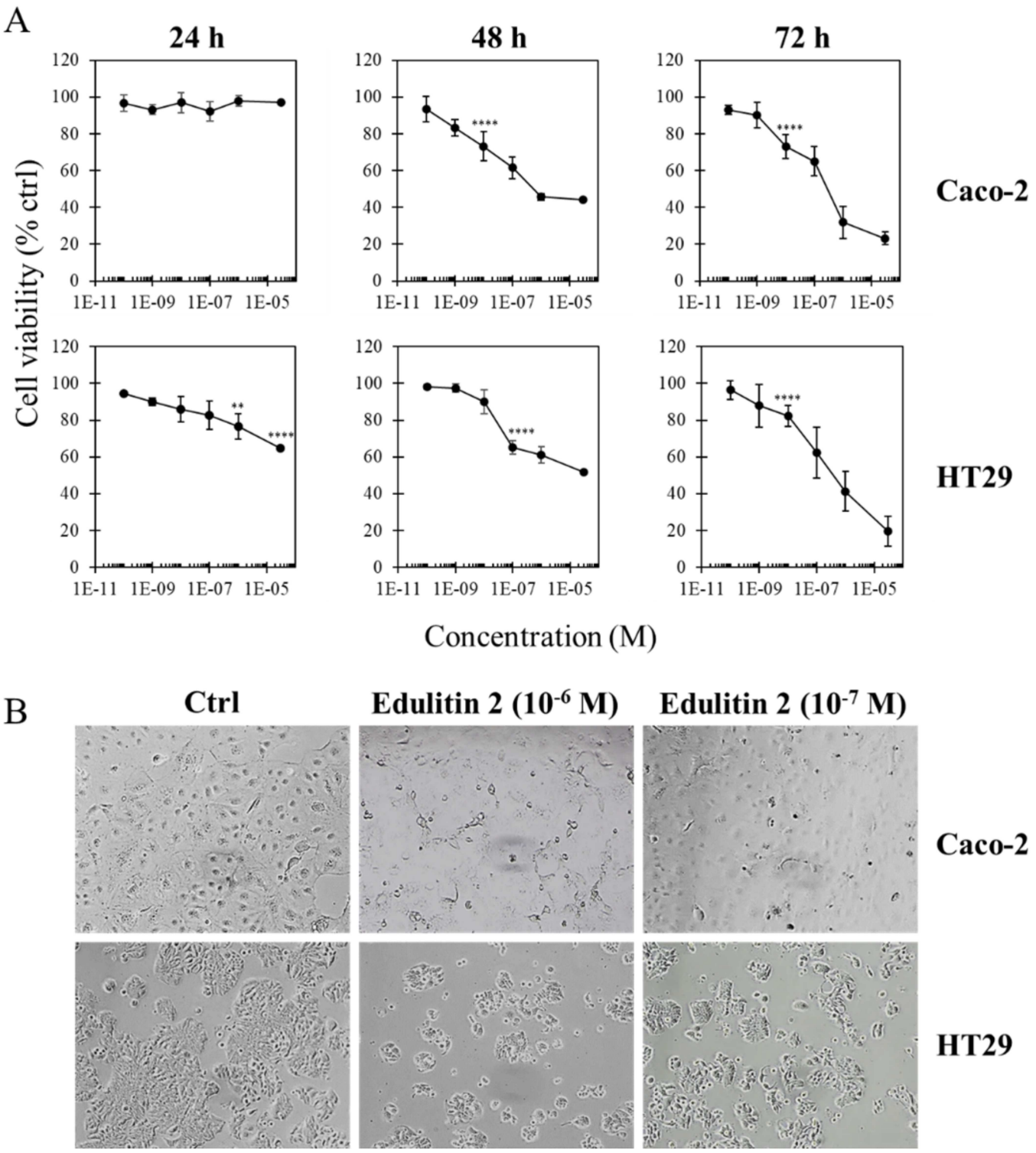

FIGURE 2 | Edulitin 2 cytotoxicity in Caco-2 and HT29 cells in concentration- and time-response experiments. (A) Cells (3×10^3/well) were treated with scalar doses of edulitin 2 (10^{-10} –3×10^{-5} M) for 24, 48 and 72 h. Cell viability was evaluated using a colorimetric assay based on MTT reduction. The results are expressed as means ± SD of three independent experiments, each conducted in triplicate. Asterisks indicate the first concentration at which a statistically significant reduction in viability was observed compared to controls. All results are plotted as relative percentage of untreated controls. Data were analyzed by ANOVA/Bonferroni test, followed by a comparison with Dunnett's test (confidence range 95%; $^{**}p < 0.01$ vs. untreated controls, $^{****}p \leq 0.0001$ vs. untreated controls). (B) Morphology changes of Caco-2 and HT29 cells through light microscopy after 72 h of treatment without (Ctrl) or with 10^{-6} or 10^{-7} M edulitin 2. The images are representative of three experiments (100× magnification).

3.2 | Edulitin 2 Reduces the Viability of Colon Adenocarcinoma Cells

The cytotoxic activity of edulitin 2 was assessed on Caco-2 and HT29 cell lines. Cells were exposed to scalar concentrations of edulitin 2 (10^{-10} – 3×10^{-5} M) and cell viability was evaluated after 24, 48 and 72 h (Figure 2A). Dose- and time-response experiments revealed that the cytotoxic effects induced by edulitin 2 progressively increased over time in both cell lines. After 24 h, edulitin 2 caused a slight reduction in cell viability only in HT29 cells at 10^{-6} M ($p < 0.01$). At 48 h, edulitin 2 significantly reduced cell viability, starting from 10^{-8} and 10^{-7} M in Caco-2 and HT29 cells, respectively. However, the reduction in cell viability was quite slow, as evidenced by the flat trend of concentration-response curves. Indeed, even at the highest tested concentration (3×10^{-5} M) edulitin 2 was able to cause a reduction in viability of just over 50%. The highest cytotoxic effect was observed after 72 h of treatment, with edulitin 2 reducing cell viability by more than 80% in both cell lines, with EC_{50}s in the 10^{-7} M range (Table 1). Microscopic analysis revealed strong cellular morphological alteration after 72 h of treatment, confirming the cytotoxic effect of edulitin 2 (Figure 2B).

TABLE 1 | Concentrations of edulitin 2 that reduce cell viability by 50% (EC_{50}), calculated by linear regression analysis of concentration-response curves.

	EC_{50} (M)		
	24 h	**48 h**	**72 h**
Caco-2	$> 3 \times 10^{-5}$	6.79×10^{-7}	2.85×10^{-7}
HT29	$> 3 \times 10^{-5}$	$> 3 \times 10^{-5}$	4.98×10^{-7}

3.3 | Edulitin 2 Affects the Epithelial Barrier Integrity Assessed by Transepithelial Electrical Resistance (TEER) Measurement in Caco-2 Monolayer

The effect of edulitin 2 on the epithelial barrier integrity was evaluated by measuring the Transepithelial Electrical Resistance (TEER) in *in vitro* models represented by Caco-2 monolayer cultured alone or on collagen. The effect of edulitin 2 on the barrier properties was monitored by TEER measurements at different timepoints from 0 to 72 h. Edulitin 2 significantly affected barrier integrity in both models (Figure 3). TEER values in Caco-2 monolayer were significantly reduced with respect to controls after 72 h of treatment with edulitin 2 at 10^{-6} M concentration, whereas in the Caco-2/collagen model TEER values started to significantly decrease after 48 h of treatment.

3.4 | Edulitin 2 Mainly Triggers Apoptosis in Caco-2 and HT29 Cells

The cell death pathways activated in edulitin 2-treated cells were evaluated by double staining with Annexin V- EGFP/PI through flow cytometry analysis. After 48 h of treatment with edulitin 2 at 10^{-6} M concentration, a significant rise in the early apoptotic population was observed in both cell lines, 39.75% (Caco-2) and 38.05% (HT29). Interestingly, only a minimal increase in late apoptosis/necroptosis and no increase in necrosis were detected in both cell lines (Figure 4A,B). To better elucidate the cell death mechanisms induced, the flow cytometry analysis was also carried out after treating Caco-2 cells for a longer time (72 h) with edulitin 2, pre-treating cells with or without the pan-caspase inhibitor Z-VAD. Annexin V-EGFP/PI double staining confirmed that edulitin 2 triggered apoptosis as the main death mechanism, even after 72 h. Notably, the

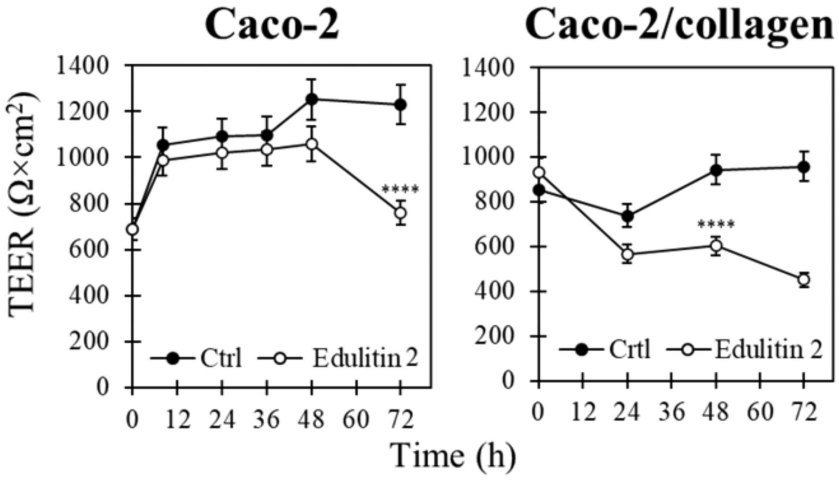

FIGURE 3 | Time-dependent impact of edulitin 2 on TEER values in Caco-2 and Caco-2/collagen culture models. Caco-2 cells (6.25×10^4 cells/cm^2) in both models were seeded on the apical chamber of Transwell inserts in 24-well plates. In Caco-2/collagen model Transwell inserts were pre-coated with 0.1 μg/ml of type 1 collagen in complete medium and incubated for 1 h at 37°C. At the end of incubation, Caco-2 cells were seeded on the apical compartment. Caco-2 cells were maintained about 10 days, replacing culture medium every 2–3 days. When TEER reached values ≥ 500 Ω × cm^2 (about 10 days), cell monolayers were treated with 10^{-6} M edulitin 2. TEER values were assessed at the indicated timepoints after edulitin 2 intoxication. Each time point represents the means ± SD of three independent experiments conducted in triplicate. Data were analyzed by ANOVA/Bonferroni test, followed by a comparison with Dunnett's test (confidence range 95%; ****$p < 0.0001$ *vs.* untreated controls). Asterisks indicate the first timepoint at which a statistically significant reduction in TEER was observed compared to controls.

A

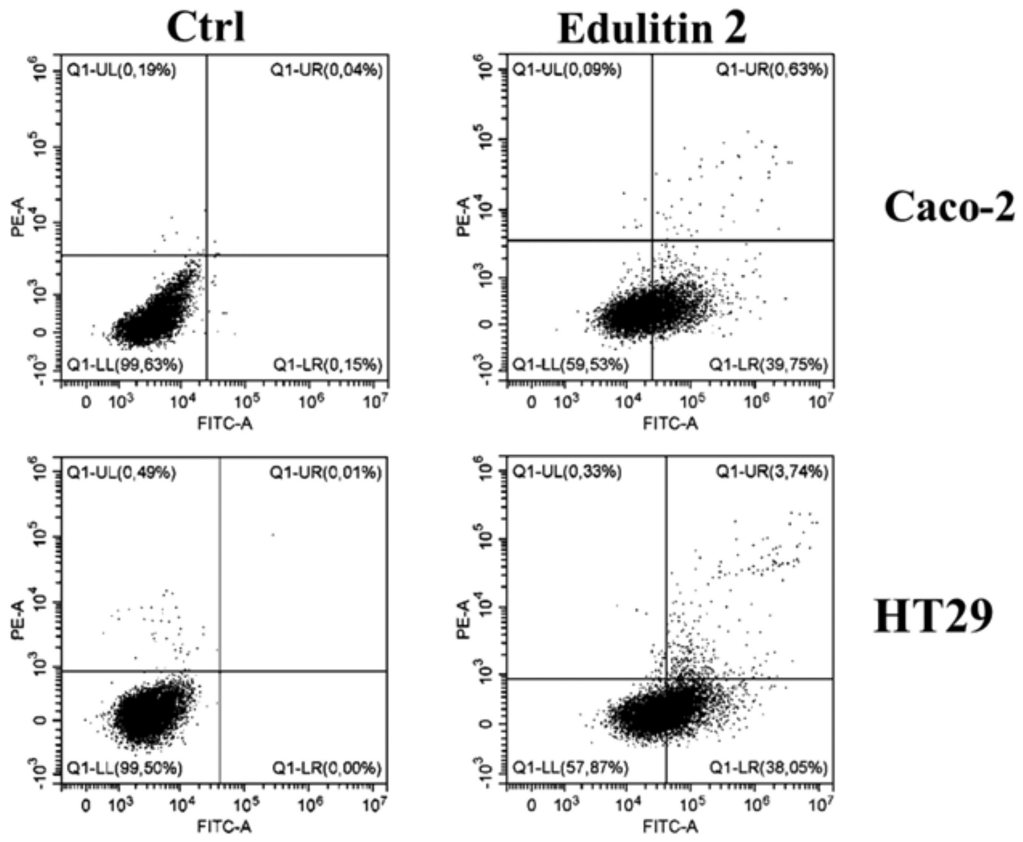

B

Caco-2		
	Ctrl	Edulitin 2
Live	99.63	59.53
Early apoptotic	0.15	39.75
Late apoptotic/ necroptotic	0.04	0.63
Necrotic	0.19	0.09

HT29		
	Ctrl	Edulitin 2
Live	99.50	57.87
Early apoptotic	0.00	38.05
Late apoptotic/ necroptotic	0.01	3.74
Necrotic	0.49	0.33

FIGURE 4 | Assessment of apoptosis, necroptosis and necrosis following Annexin V-EGFP/PI staining and flow cytometric analysis. (A) Caco-2 and HT29 cells (4×10^5 cells/well) were cultured for 48 h without (Ctrl) or with 10^{-6} M edulitin 2. Apoptotic, necroptotic and necrotic cells were subsequently evaluated by flow cytometry. Representative plots of Annexin V-EGFP (FITC channel)/PI (PE channel) staining of Caco-2 and HT29 cells are shown. Early apoptotic (PI-negative and EGFP-positive) cells are in the lower right quadrant, late apoptotic/necroptotic (PI-positive and EGFP-positive) are in the upper right quadrant, necrotic cells (PI-positive and EGFP-negative) are in the upper left quadrant. The dot plots are representative of three independent experiments, each performed in triplicate. (B) In the table the percentages of live, early apoptotic, late apoptotic/necroptotic and necrotic cells after edulitin 2 intoxication are reported.

pre-treatment with Z-VAD completely protected cells from edulitin 2-induced apoptosis (Figure 5A,B). These results were confirmed by the viability experiments; the inhibitors Z-VAD and necrostatin-1 significantly rescued cells by edulitin 2-induced cell death (Figure 5C). These data strongly indicate that edulitin 2 promotes cell death primarily through the activation of a caspase-dependent apoptotic pathway. The partial protective effect observed upon necrostatin-1 treatment suggests a possible contribution of necroptotic pathway after long incubation time (72 h).

3.5 | Edulitin 2 Affects the Ribosomes of *T. harzianum*, but Not Those of *E. coli*

Like other RL-Ps, the target of edulitin 2 is the SRL structure (Landi et al. 2021), a critical region for ribosome function and elongation factors interaction in both prokaryotes and eukaryotes (Szewczak et al. 1993). However, this region shows different structural features in prokaryotic and eukaryotic rRNA (García-Mayoral et al. 2005; Seggerson and Moore 1998). In light of this, the Endo assay was carried out on both eukaryotic (*T. harzianum, ascomycete fungus*)

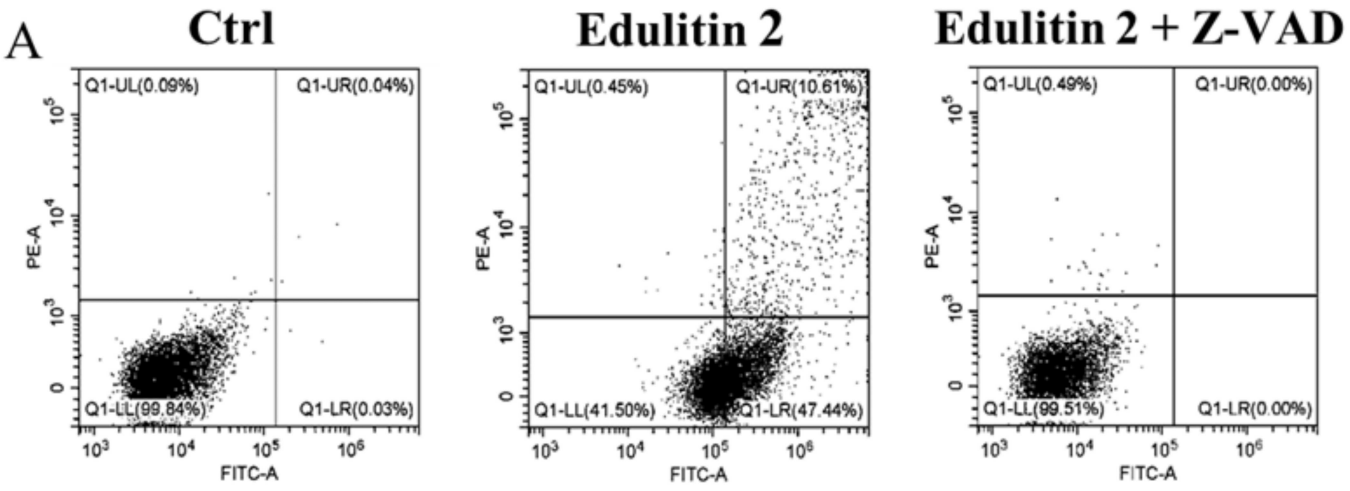

B

	Ctrl	Edulitin 2	Edulitin 2 + Z-VAD
Live	99.84	41.50	99.51
Early apoptotic	0.03	47.44	0.00
Late apoptotic/ necroptotic	0.04	10.61	0.00
Necrotic	0.09	0.45	0.49

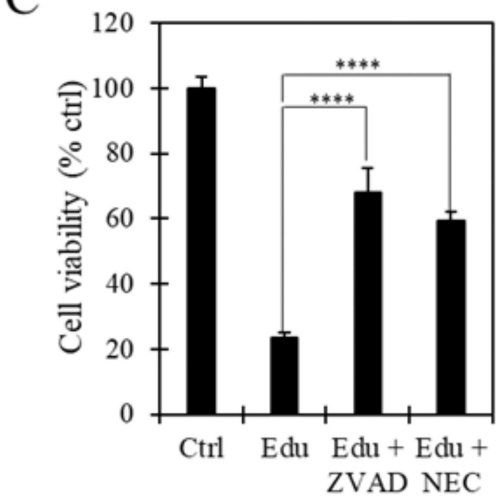

FIGURE 5 | Evaluation of cell death mechanisms after edulitin 2 intoxication on Caco-2 cells pre-treated with cell death inhibitors. (A) Caco-2 cells (4×10^5 cells/well) were treated with 10^{-6} M edulitin 2, without or in presence of 100 μM pan-caspase inhibitor Z-VAD. Cells were pre-incubated for 3 h with Z-VAD before edulitin 2 incubation. After 72 h, apoptotic, necroptotic and necrotic cells were evaluated by flow cytometry. Representative plots of Annexin V-EGFP (FITC channel)/PI (PE channel) staining of Caco-2 cells are shown. Early apoptotic (PI-negative and EGFP-positive) cells are in the lower right quadrant, late apoptotic/necroptotic (PI-positive and EGFP-positive) are in the upper right quadrant, necrotic cells (PI-positive and EGFP-negative) are in the upper left quadrant. (B) In the table the percentages of live, early apoptotic, late apoptotic/necroptotic and necrotic cells after edulitin 2 intoxication (alone or with Z-VAD) are reported. (C) The protective effects of Z-VAD and of the necroptosis inhibitor necrostatin-1 (NEC) were evaluated on Caco-2 cells. Cells (3×10^3/well) were pre-treated with 100 μM Z-VAD or NEC for 3 h before edulitin 2 (Edu) treatment. Cells were then treated with edulitin 2 for 72 h. Cell viability was evaluated using a colorimetric assay based on MTT reduction. The results are expressed as means ± S.D. of three independent experiments, each conducted in triplicate. Data were analyzed by the Mann–Whitney *U* test (confidence range 95%; ****$p < 0.0001$ *vs.* RL-P-treated samples).

and prokaryotic (*E. coli*) ribosomes, in order to gain insight into the edulitin 2 substrate specificity. As shown in Figure 6, edulitin 2 was able to release the α-fragment, when incubated with *T. harzianum*, while it was unable to damage *E. coli* ribosomes.

3.6 | Edulitin 2 Does Not Affect Intestinal Microorganisms

The growth of pure cultures of intestinal microbes in the presence or absence of edulitin 2 was monitored by optical density measurements over 24 h. The growth of Gram-positive or Gram-negative bacteria, as well as microscopic fungi of intestinal origin was not affected when supplemented with concentrations of edulitin 2 from 1.43×10^{-7} to 1.43×10^{-5} M (2.0 up to 200 μg/mL; data not shown).

The effects of edulitin 2 were also analyzed using intestinal microbial consortia in an *in vitro* cultivation-based system (Landi et al. 2025; Rettedal et al. 2014). Human fecal samples were collected from healthy children ($n = 3$) not under antibiotic or probiotic treatment for at least 3 months before the sampling day. An aliquot of each sample (200 mg) was used to immediately extract total DNA (Control group) while other aliquots of the same weight of each sample were independently resuspended in MGAM medium (see Materials and Methods), supplemented (Treated group) or not (Untreated group) with 2.86×10^{-5} M (400 μg/mL) of edulitin 2. Samples were incubated in anaerobic conditions for 3 days and total DNA of each sample was extracted and subjected to 16S rRNA gene sequencing, as previously reported (Landi et al. 2025; Milani et al. 2013).

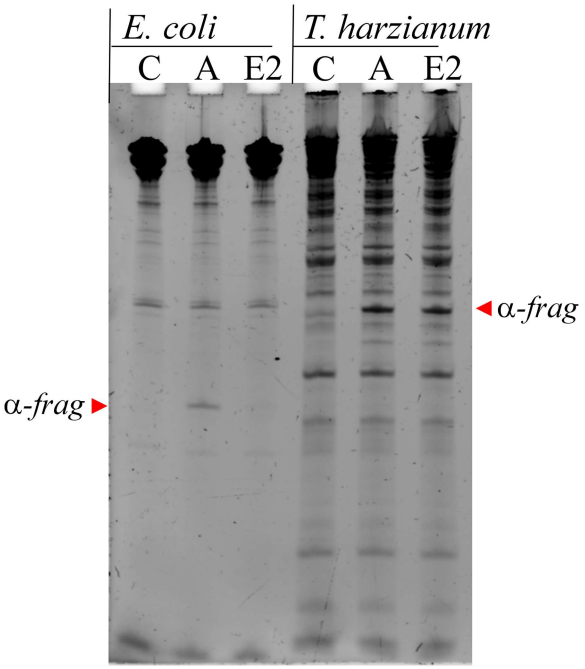

FIGURE 6 | Effect of edulitin 2 (E2) on *T. harzianum* or *E. coli* ribosomes compared to ageritin (A). The arrows indicate the diagnostic α-fragment released as a result of RL-P enzymatic action revealed by Endo's assay.

Ten out of the seventeen bacterial phyla originally present in the fecal samples were recovered after cultivation with the phyla no longer present being mostly strict anaerobes, as previously reported (Landi et al. 2025). At the family level, 36 out of 62 originally present families were found after cultivation in agreement with previous reports on this in vitro cultivation approach (Rettedal et al. 2014).

Statistical analyses (see Materials and Methods) indicated the increased abundance of members of the *Patescibacteria* phylum in the edulitin 2-treated group as the only significant difference at the phylum level (Table S2**).** Similarly, at the genus level only one difference between the two experimental groups appeared statistically significant, with members of the *Desulfotomaculum* genus more abundant in the edulitin 2-treated group (Table S3). These small differences consist of increased number of bacteria in the edulitin 2-treated group, supporting the conclusion that the enzyme does not have any anti-bacterial activity.

In line with this, the analysis of alpha diversity (Observed ASVs, Chao1, and Shannon indices; Figure 7A) and beta diversity (PCoA plot; Figure 7B) revealed no significant differences after edulitin 2-treatment. In summary, the RL-P exerted no influence on intestinal microorganisms under either pure culture conditions or simulated intestinal consortia.

4 | Discussion

The consumption of *B. edulis* dates back to the time of the ancient Greeks and Romans, who influenced the cooking method and made this mushroom popular due to its intense flavor and enveloping aroma (Hobbs 2021). In addition, empirical evidence supports that *B. edulis* fruiting bodies promote beneficial effects on human health (Casado-Hidalgo et al. 2025; Tan et al. 2022). In light of this, this mushroom plays a significant role in the culture and traditions of many European regions. Nowadays, significant research into the beneficial effects of consuming *B. edulis* confirms the empirical evidence, highlighting that *B. edulis* fruiting bodies are a rich reservoir of many intriguing bioactive molecules with immune-modulating, tumor-suppressing, antioxidant and liver-protective effects (Casado-Hidalgo et al. 2025; Quero et al. 2024).

In this study we investigated the antiproliferative activity of edulitin 2 on Caco-2 and HT29 cells, which are widely recognized as standardized and reliable in vitro models of human colon carcinoma, due to their well-characterized morphological and functional properties. Considering the increasing consumption of uncooked *B. edulis* mushrooms in fresh salads (Chefbikeski 2017) and the low susceptibility of edulitin 2 to proteases such as pepsin and trypsin (Landi et al. 2021), a direct action of this RL-P on tumor cells in the gastrointestinal tract may be possible. Our results revealed that edulitin 2 efficiently reduced cell viability in concentration- and time-response experiments on both tested cell lines. The effect was particularly evident after 72 h of incubation, with EC_{50} values in the 10^{-7} M range for both cell lines. The slight difference in temporal sensitivity to edulitin 2 observed between Caco-2 and HT29 cells may be related to the distinct biological features of the two intestinal epithelial models. Caco-2 cells undergo spontaneous differentiation toward an enterocyte-like phenotype, characterized by the formation of tight junctions and a more pronounced barrier function, which may delay their cytotoxic susceptibility to drugs or other toxics (Sambuy et al. 2005). In contrast, HT29 cells are less differentiated and display a more proliferative phenotype than Caco-2 cells, which may account for their higher sensitivity to edulitin 2 at 24 h (Martínez-Maqueda et al. 2015). However, a prolonged exposure to edulitin 2 (72 h) resulted in comparable cytotoxic effects in both cell lines.

TEER is a widely accepted, non-invasive method for monitoring the formation and maintenance of tight junctions in epithelial monolayers, providing real-time insights into barrier function and cellular differentiation. The use of collagen-coated inserts in Caco-2/collagen system mimics more closely the epithelial barrier formation and promotes a more physiological relevance compared to the conventional Caco-2 monolayer (Ferreira et al. 2025). Edulitin 2 affected the integrity of the epithelial barrier in our intestinal models. In the Caco-2 monolayer, grown alone or on a surface of collagen gel, edulitin 2 significantly decreased TEER values after 72 h and 48 h, respectively. The weakening of the Caco-2 epithelial barrier tight junctions suggests that edulitin 2 could increase the paracellular permeability in the tumor mass, thereby favoring the entry of other antineoplastic drugs (Zhang et al. 2024). The different TEER kinetics observed between the Caco-2 monolayer and Caco-2/collagen models after edulitin 2 treatment may be attributed to the distinct microenvironment provided by collagen. Collagen is known to influence cell adhesion, cytoskeletal organization and tight junction dynamics, thereby modulating barrier properties and cellular responsiveness to external stimuli. In the Caco-2/collagen system, this may render tight junctions more susceptible to early perturbations, resulting in lower TEER values than those reported in the Caco-2 monolayer (Linz et al. 2020).

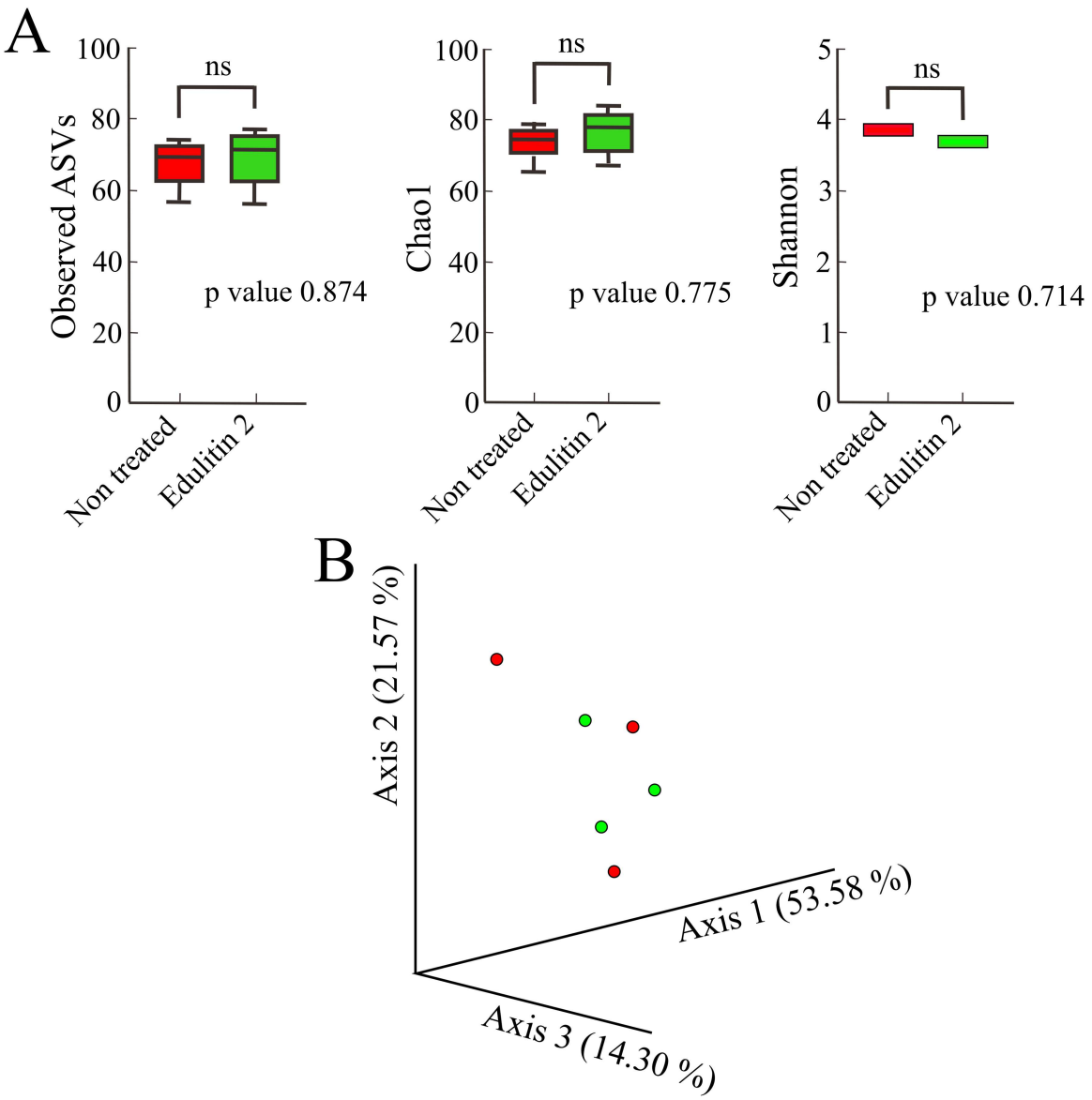

FIGURE 7 | The impact of edulitin 2 on intestinal microorganisms. Alpha and beta diversity were assessed using 16S rRNA gene sequencing data from fecal-derived cultures, comparing Untreated samples with those Treated with edulitin 2 (2.86×10^{-5} M corresponding to 400 μg/mL). (A) Alpha diversity, evaluated through Observed ASV richness, Chao1, and Shannon indices, showed no significant differences between groups. Statistical comparisons of alpha diversity were performed using an unpaired Student's *t*-test in GraphPad Prism 9 (San Diego, CA). (B) The principal coordinates analysis (PCoA) plot revealed no distinct separation between the groups. In red non treated samples, in green samples treated with edulitin 2.

By examining the mechanisms of cell death induced by edulitin 2, it is possible to demonstrate that this enzyme is able to kill cells mainly by triggering apoptosis in both Caco-2 and HT29 cells. After 48 h, most of the treated cells showed signs of early-stage apoptosis. A small percentage of cells showed late-stage apoptosis, which became more evident after 72 h of treatment. Interestingly, edulitin 2 did not significantly induce necrosis in treated cells. The predominance of apoptosis over necrosis upon edulitin 2 treatment may suggest a reduced probability of inflammation-associated damage in vivo, as apoptosis is a well-known immunologically silent process (Bock and Riley 2023). This represents a major advantage for a potential clinical use of edulitin 2. The viability of cells treated with edulitin 2 was significantly improved by pre-treatment with the pan-caspase inhibitor Z-VAD and the necroptosis inhibitor necrostatin-1, confirming the involvement of mainly apoptosis and to a lesser extent necroptosis in edulitin 2-induced cytotoxicity.

Edulitin 2 is only minimally affected by proteases in an in vitro digestibility system (Landi et al. 2021) and it is therefore likely to safely cross the stomach, reaching the intestine in an active form and affecting the microbial composition of the gastrointestinal tract (gut microbiota). This harbors a complex ecosystem of microorganisms (viruses, bacteria, fungi, protozoans and archaea), which have co-evolved with humans and differ in composition and function based on the age, sex, race/ethnicity, and diet of their host (Lozupone et al. 2012). Microbial communities of gut microbiota are in symbiosis with the host, contributing to the human organism homeostasis and regulating human immune function (Hou et al. 2022). Due to the strict relationship within the gut microbiota, any change of one group

of microorganisms may affect the relative abundance of other groups, altering the balance of gut microbiota and potentially leading to intestinal and extraintestinal diseases (Lozupone et al. 2012; Peroni et al. 2020). Edulitin 2 does not have any antibacterial activity in vitro (see paragraph 3.5) or in vivo on pure cultures of bacteria or yeasts (see paragraph 3.6), but it damages in vitro fungal ribosomes (see paragraph 3.5) and could, therefore, alter the overall composition of the gut microbiota. Such possibility was evaluated by analyzing the effects of edulitin 2 on microbial consortia simulating the gut microbiota. No statistically significant effects were observed in the composition of the gut microbiota after the treatment with edulitin 2. Thus, the consumption of *B. edulis* could have beneficial effects also for the presence of bioactive proteins/enzymes, such as edulitin 2 that has antiproliferative activities against tumor cells without negatively effecting the composition of the gut microbiota.

5 | Conclusions

This study demonstrates that edulitin 2, a bioactive protein from *B. edulis*, exerts significant anti-tumor effects in our in vitro colon cancer model. Edulitin 2 exhibits cytotoxic effects, primarily inducing apoptosis, with limited involvement of necroptosis and no necrosis, supporting its potential therapeutic relevance due to the low risk of inflammation-associated damage. Furthermore, edulitin 2 compromises the integrity of the epithelial barrier, resulting in enhanced paracellular permeability within the tumor mass. Interestingly, edulitin 2 does not significantly alter the composition of gut microbiota consortia.

Overall, these results identify edulitin 2 as a promising bioactive compound that combines effective cytotoxic activity against tumor cells with a favorable safety profile toward the intestinal microbiota. These properties warrant further investigation to more precisely define edulitin 2 tumor selectivity, to evaluate its safety toward non-transformed intestinal epithelial cells and to assess its behavior in relevant in vivo models. Such studies will be essential to explore the potential biomedical applications of edulitin 2, particularly in the context of loco-regional administration strategies or its incorporation into immunotoxin-based approaches for the selective elimination of unwanted cells.

Author Contributions

Massimo Bortolotti: investigation, methodology, formal analysis. **Sara Ragucci:** investigation, methodology, formal analysis. **Federica Falà:** investigation, methodology, formal analysis. **Anella Saggese:** investigation, methodology, formal analysis. **Francesco Biscotti:** investigation, methodology, formal analysis. **Ylenia De Luca:** investigation, methodology, formal analysis. **Nicola Landi:** investigation, methodology, formal analysis. **Paolo V. Pedone:** investigation, methodology, formal analysis. **Andrea Bolognesi:** funding acquisition, writing – review and editing, data curation. **Ezio Ricca:** funding acquisition, writing – review and editing, data curation. **Letizia Polito:** writing – review and editing, data curation, writing – original draft, supervision. **Antimo Di Maro:** conceptualization, writing – original draft, writing – review and editing, data curation, supervision.

Acknowledgments

This study was made possible by the care and abnegation of all participants. The study was provided by grants from the "Ministero dell'Universita e della Ricerca" (MUR; Prin 2022 PNRR, entitled "Direct or indirect effects of protein synthesis inhibitor enzymes from edible plants and mushrooms on intestinal health and microbiota," Prot. P2022YERKR). It was also supported by the research project "Potentiating the Italian Capacity for Structural Biology Services in Instruct-ERIC," acronym "ITACA.SB" (Project No. IR0000009, CUP B53C22001790006), funded by the European Union's NextGenerationEU under the MUR call 3264/2021 PNRR M4/C2/L3.1.1.

Conflicts of Interest

The authors declare no conflicts of interest.

Data Availability Statement

The data that support the findings of this study are available from the corresponding author upon reasonable request.

References

Biscotti, F., M. Bortolotti, F. Falà, A. Di Maro, A. Bolognesi, and L. Polito. 2025. "Ricin Toxicity to Intestinal Cells Leads to Multiple Cell Death Pathways Mediated by Oxidative Stress." *Toxins* 17, no. 8: 400. https://doi.org/10.3390/toxins17080400.

Bock, F. J., and J. S. Riley. 2023. "When Cell Death Goes Wrong: Inflammatory Outcomes of Failed Apoptosis and Mitotic Cell Death." *Cell Death & Differentiation* 30, no. 2: 293–303. https://doi.org/10.1038/s41418-022-01082-0.

Bortolotti, M., F. Biscotti, A. Zanello, L. Polito, and A. Bolognesi. 2023. "Heterophyllin: A New Adenia Toxic Lectin With Peculiar Biological Properties." *Toxins* 16, no. 1: 1. https://doi.org/10.3390/toxins16010001.

Bortolotti, M., A. Zanello, L. Serra, F. Biscotti, L. Polito, and A. Bolognesi. 2023. "Plant Toxins as Potential Alternatives to Botulinum Toxin for Eye-Movement Disorder Therapy." *Stresses* 3, no. 1: 270–281. https://doi.org/10.3390/stresses3010020.

Bovi, M., M. E. Carrizo, S. Capaldi, et al. 2011. "Structure of a Lectin With Antitumoral Properties in King Bolete (*Boletus Edulis*) Mushrooms." *Glycobiology* 21, no. 8: 1000–1009. https://doi.org/10.1093/glycob/cwr012.

Bovi, M., L. Cenci, M. Perduca, et al. 2013. "Bel β-trefoil: A Novel Lectin With Antineoplastic Properties in King Bolete (*Boletus Edulis*) Mushrooms." *Glycobiology* 23, no. 5: 578–592. https://doi.org/10.1093/glycob/cws164.

Buglione, M., E. Ricca, S. Petrelli, et al. 2022. "Gut Microbiota Plasticity in Insular Lizards under Reversed Island Syndrome." *Scientific Reports* 12, no. 1: 12682. https://doi.org/10.1038/s41598-022-16955-0.

Callahan, B. J., P. J. McMurdie, M. J. Rosen, A. W. Han, A. J. A. Johnson, and S. P. Holmes. 2016. "DADA2: High-Resolution Sample Inference From Illumina Amplicon Data." *Nature Methods* 13, no. 7: 581–583. https://doi.org/10.1038/nmeth.3869.

Casado-Hidalgo, G., P. Cebollada, J. Cano-Lou, et al. 2025. "*Boletus edulis* as a Healthy and Prized Edible Mushroom: Analysis of Bioactive Compounds and In Vitro Functional Properties." *Applied Food Research* 5, no. 2: 101342. https://doi.org/10.1016/j.afres.2025.101342.

Chambery, A., M. Pisante, A. Di Maro, et al. 2007. "Invariant Ser211 Is Involved in the Catalysis of PD-L4, Type I Rip From *Phytolacca Dioica* Leaves." *Proteins: Structure, Function, and Bioinformatics* 67, no. 1: 209–218. https://doi.org/10.1002/prot.21271.

Chefbikeski. 2017. Insalata di Porcini Crudo – Raw Porcini Mushroom Salad. Italian Food, Wine, and Travel. Retrieved 20/11/2025 from https://www.chefbikeski.com/insalata-di-porcini-crudo-raw-porcini-mushroom-salad/.

Correll, C. C., A. Munishkin, Y. L. Chan, Z. Ren, I. G. Wool, and T. A. Steitz. 1998. "Crystal Structure of the Ribosomal RNA Domain Essential for Binding Elongation Factors." *Proceedings of the National*

Academy of Sciences 95, no. 23: 13436–13441. https://doi.org/10.1073/pnas.95.23.13436.

Ferreira, B., C. Ferreira, C. Martins, et al. 2025. "Establishment of a 3D Multi-Layered *In Vitro* Model of Inflammatory Bowel Disease." *Journal of Controlled Release* 377: 675–688. https://doi.org/10.1016/j.jconrel.2024.11.070.

García-Mayoral, F., L. García-Ortega, E. Álvarez-García, M. Bruix, J. G. Gavilanes, and Á. Martínez del Pozo. 2005. "Modeling the Highly Specific Ribotoxin Recognition of Ribosomes." *FEBS Letters* 579, no. 30: 6859–6864. https://doi.org/10.1016/j.febslet.2005.11.027.

Hall, I. R., A. J. E. Lyon, Y. Wang, and L. Sinclair. 1998. "Ectomycorrhizal Fungi With Edible Fruiting Bodies 2. *Boletus Edulis*." *Economic Botany* 52, no. 1: 44–56. https://doi.org/10.1007/BF02861294.

Herrero-Galán, E., L. García-Ortega, M. Olombrada, et al. 2013. "Hirsutellin A: A Paradigmatic Example of the Insecticidal Function of Fungal Ribotoxins." *Insects* 4, no. 3: 339–356. https://doi.org/10.3390/insects4030339.

Hobbs, C. 2021. *Christopher Hobbs Medicinal Mushrooms, The Essential Guide*. Storey Publishing, LLC.

Hou, K., Z. X. Wu, X. Y. Chen, et al. 2022. "Microbiota in Health and Diseases." *Signal Transduction and Targeted Therapy* 7, no. 1: 135. https://doi.org/10.1038/s41392-022-00974-4.

Landi, N., M. Bortolotti, S. Ragucci, et al. 2025. "Effects of Indicitin, a Novel Ribosome-Targeting Enzyme From Milky Mushrooms, on Four Human Cell Lines and the Gut Microbiota." *Food & Function* 16: 9160–9173. https://doi.org/10.1039/d5fo03851k.

Landi, N., M. Grundner, S. Ragucci, et al. 2022. "Characterization and Cytotoxic Activity of Ribotoxin-Like Proteins From the Edible Mushroom *Pleurotus Eryngii*." *Food Chemistry* 396: 133655. https://doi.org/10.1016/j.foodchem.2022.133655.

Landi, N., S. Pacifico, S. Ragucci, et al. 2017. "Purification, Characterization and Cytotoxicity Assessment of Ageritin: The First Ribotoxin From the Basidiomycete Mushroom *Agrocybe Aegerita*." *Biochimica et Biophysica Acta (BBA) - General Subjects* 1861, no. 5 pt. A: 1113–1121. https://doi.org/10.1016/j.bbagen.2017.02.023.

Landi, N., S. Ragucci, R. Culurciello, et al. 2021. "Ribotoxin-Like Proteins From *Boletus Edulis*: Structural Properties, Cytotoxicity and *in Vitro* Digestibility." *Food Chemistry* 359: 129931. https://doi.org/10.1016/j.foodchem.2021.129931.

Lemieszek, M. K., P. S. Marques, M. Ribeiro, et al. 2019. "Mushroom Small Rnas as Potential Anticancer Agents: A Closer Look at Cantharellus Cibarius Proapoptotic and Antiproliferative Effects in Colon Cancer Cells." *Food & Function* 10, no. 5: 2739–2751. https://doi.org/10.1039/c8fo02378f.

Lemieszek, M. K., M. Ribeiro, G. Marques, F. M. Nunes, P. Pożarowski, and W. Rzeski. 2017. "New Insights into the Molecular Mechanism of Boletus Edulis Ribonucleic Acid Fraction (BE3) Concerning Antiproliferative Activity on Human Colon Cancer Cells." *Food & Function* 8, no. 5: 1830–1839. https://doi.org/10.1039/c6fo01626j.

Linz, G., S. Djeljadini, L. Steinbeck, G. Köse, F. Kiessling, and M. Wessling. 2020. "Cell Barrier Characterization in Transwell Inserts by Electrical Impedance Spectroscopy." *Biosensors & Bioelectronics* 165: 112345. https://doi.org/10.1016/j.bios.2020.112345.

Lozupone, C. A., J. I. Stombaugh, J. I. Gordon, J. K. Jansson, and R. Knight. 2012. "Diversity, Stability and Resilience of the Human Gut Microbiota." *Nature* 489, no. 7415: 220–230. https://doi.org/10.1038/nature11550.

Martínez-Maqueda, D., B. Miralles, and I. Recio. 2015. "HT29 Cell Line." In *The Impact of Food Bioactives on Health: in vitro and ex vivo models*, edited by K. Verhoeckx, P. Cotter, I. López-Expósito, C. Kleiveland, T. Lea, A. Mackie, T. Requena, D. Swiatecka, and H. Wichers, 113–124. Springer International Publishing. https://doi.org/10.1007/978-3-319-16104-411.

Martínez-Ruiz, A., L. García-Ortega, R. Kao, et al. 2001. "[21] - RNase U2 and α-Sarcin: A Study of Relationships." In *Methods in Enzymology*, edited by A. W. Nicholson, 341, 335–351. Academic Press. https://doi.org/10.1016/S0076-6879(01)41162-1.

Mayirnao, H.-S., K. Sharma, P. Jangir, S. Kaur, and R. Kapoor. 2025. "Mushroom-Derived Nutraceuticals in the 21st Century: An Appraisal and Future Perspectives." *Journal of Future Foods* 5, no. 4: 342–360. https://doi.org/10.1016/j.jfutfo.2024.07.013.

Milani, C., A. Hevia, E. Foroni, et al. 2013. "Assessing the Fecal Microbiota: An Optimized Ion Torrent 16S rRNA Gene-Based Analysis Protocol." *PLoS One* 8, no. 7: e68739. https://doi.org/10.1371/journal.pone.0068739.

Olombrada, M., R. Lázaro-Gorines, J. López-Rodríguez, et al. 2017. "Fungal Ribotoxins: A Review of Potential Biotechnological Applications." *Toxins* 9, no. 2: 71. https://doi.org/10.3390/toxins9020071.

Olombrada, M., Á. Martínez-del-Pozo, P. Medina, F. Budia, J. G. Gavilanes, and L. García-Ortega. 2014. "Fungal Ribotoxins: Natural Protein-Based Weapons Against Insects." *Toxicon* 83: 69–74. https://doi.org/10.1016/j.toxicon.2014.02.022.

Peroni, D. G., G. Nuzzi, I. Trambusti, M. E. Di Cicco, and P. Comberiati. 2020. "Microbiome Composition and Its Impact on the Development of Allergic Diseases." *Frontiers in immunology* 11: 700. https://doi.org/10.3389/fimmu.2020.00700.

Pietkiewicz, S., J. H. Schmidt, and I. N. Lavrik. 2015. "Quantification of Apoptosis and Necroptosis at the Single Cell Level by a Combination of Imaging Flow Cytometry With Classical Annexin V/Propidium Iodide Staining." *Journal of Immunological Methods* 423: 99–103. https://doi.org/10.1016/j.jim.2015.04.025.

Polito, L., A. Djemil, and M. Bortolotti. 2016. "Plant Toxin-Based Immunotoxins for Cancer Therapy: A Short Overview." *Biomedicines* 4, no. 2: 12. https://doi.org/10.3390/biomedicines4020012.

Quero, J., M. Paesa, C. Morales, et al. 2024. "Biological Properties of *Boletus Edulis* Extract on Caco-2 Cells: Antioxidant, Anticancer, and Anti-Inflammatory Effects." *Antioxidants* 13, no. 8: 908. https://doi.org/10.3390/antiox13080908.

Ragucci, S., N. Landi, R. Russo, et al. 2021. "Ageritin From Pioppino Mushroom: The Prototype of Ribotoxin-Like Proteins, a Novel Family of Specific Ribonucleases in Edible Mushrooms." *Toxins* 13, no. 4: 263. https://doi.org/10.3390/toxins13040263.

Rettedal, E. A., H. Gumpert, and M. O. A. Sommer. 2014. "Cultivation-Based Multiplex Phenotyping of Human Gut Microbiota Allows Targeted Recovery of Previously Uncultured Bacteria." *Nature Communications* 5: 4714. https://doi.org/10.1038/ncomms5714.

Sambuy, Y., I. De Angelis, G. Ranaldi, M. L. Scarino, A. Stammati, and F. Zucco. 2005. "The Caco-2 Cell Line as a Model of the Intestinal Barrier: Influence of Cell and Culture-Related Factors on Caco-2 Cell Functional Characteristics." *Cell Biology and Toxicology* 21, no. 1: 1–26. https://doi.org/10.1007/s10565-005-0085-6.

Seggerson, K., and P. B. Moore. 1998. "Structure and Stability of Variants of the Sarcin-Ricin Loop of 28S Rrna: Nmr Studies of the Prokaryotic Srl and a Functional Mutant." *RNA* 4, no. 10: 1203–1215. https://doi.org/10.1017/s1355838298980773.

Sharma, P., V. Jhawat, P. Mathur, and R. Dutt. 2022. "Innovation in Cancer Therapeutics and Regulatory Perspectives." *Medical Oncology* 39, no. 5: 76. https://doi.org/10.1007/s12032-022-01677-0.

Sitta, N., and M. Floriani. 2008. "Nationalization and Globalization Trends in the Wild Mushroom Commerce of Italy With Emphasis on Porcini (*Boletus Edulis* and Allied Species)." *Economic Botany* 62, no. 3: 307–322. https://doi.org/10.1007/s12231-008-9037-4.

Sivamaruthi, B. S., N. Sisubalan, P. Kesika, I. Sureka, and C. Chaiyasut. 2024. "A Concise Review of the Nutritional Profiles, Microbial Dynamics, and Health Impacts of Fermented Mushrooms." *Journal of*

Food Science 89, no. 7: 3973–3994. https://doi.org/10.1111/1750-3841.17172.

Sun, J., T. B. Ng, H. Wang, and G. Zhang. 2014. "A Novel Hemagglutinin With Antiproliferative Activity Against Tumor Cells From the Hallucinogenic Mushroom Boletus Speciosus." *BioMed Research International* 2014: 340467. https://doi.org/10.1155/2014/340467.

Szewczak, A. A., P. B. Moore, Y. L. Chang, and I. G. Wool. 1993. "The Conformation of the Sarcin/Ricin Loop From 28S Ribosomal RNA." *Proceedings of the National Academy of Sciences* 90, no. 20: 9581–9585. https://doi.org/10.1073/pnas.90.20.9581.

Tan, Y., N. K. Zeng, and B. Xu. 2022. "Chemical Profiles and Health-Promoting Effects of Porcini Mushroom (Boletus Edulis): A Narrative Review." *Food Chemistry* 390: 133199. https://doi.org/10.1016/j.foodchem.2022.133199.

Tayyrov, A., S. Azevedo, R. Herzog, et al. 2019. "Heterologous Production and Functional Characterization of Ageritin, a Novel Type of Ribotoxin Highly Expressed During Fruiting of the Edible Mushroom *Agrocybe Aegerita*." *Applied and Environmental Microbiology* 85, no. 21: e01549-01519. https://doi.org/10.1128/aem.01549-19.

Wool, I. G., A. Glück, and Y. Endo. 1992. "Ribotoxin Recognition of Ribosomal Rna and a Proposal for the Mechanism of Translocation." *Trends in Biochemical Sciences* 17, no. 7: 266–269. https://doi.org/10.1016/0968-0004(92)90407-z.

Zhang, L. Z., R. J. Du, D. Wang, et al. 2024. "Enteral Route Nanomedicine for Cancer Therapy." *International Journal of Nanomedicine* 19: 9889–9919. https://doi.org/10.2147/ijn.S482329.

Zhang, Y., R. Zhou, F. Liu, and T. B. Ng. 2021. "Purification and Characterization of a Novel Protein With Activity Against Non-Small-Cell Lung Cancer *In Vitro* and *In Vivo* From the Edible Mushroom *Boletus Edulis*." *International Journal of Biological Macromolecules* 174: 77–88. https://doi.org/10.1016/j.ijbiomac.2021.01.149.

Supporting Information

Additional supporting information can be found online in the Supporting Information section.

Table S1: NCBI Sequence Read Archive (SRA) accession numbers of data generated in this study (BioProject number PRJNA1291050).

Table S1: NCBI Sequence Read Archive (SRA) accession numbers of data generated in this study (BioProject number PRJNA1291050).

Table S3: Average abundance of bacteria at the genus level of edulitin 2-Treated and Untreated groups.